Research Communication

Enzymatic Processing by MMP-2 and MMP-9 of Wild-type and Mutated Mouse β-Dystroglycan

Diego Sbardella[1,2], Rosanna Inzitari[3], Federica Iavarone[3*], Magda Gioia[1,2], Stefano Marini[1,2], Francesca Sciandra[4], Massimo Castagnola[3], Philippe E. Van den Steen[5], Ghislain Opdenakker[5], Bruno Giardina[3], Andrea Brancaccio[4], Massimo Coletta[1,2], and Manuela Bozzi[3]
[1]*Dipartimento di Scienze Cliniche e Medicina Traslazionale, Università di Roma Tor Vergata, Roma, Italy*
[2]*CIRCMSB, Bari, Italy*
[3]*Istituto di Biochimica e Biochimica Clinica, Università Cattolica del Sacro Cuore, Roma, Italy*
[4]*Istituto di Chimica del Riconoscimento Molecolare (CNR), Roma, Italy*
[5]*Rega Institute, Catholic University of Leuven, Leuven, Belgium*

Summary

Dystroglycan (DG) is a membrane-associated protein complex formed by two noncovalently linked subunits, α-DG, a highly glycosylated extracellular protein, and β-DG, a transmembrane protein. The interface between the two DG subunits, which is crucial to maintain the integrity of the plasma membrane, involves the C-terminal domain of α-DG and the N-terminal extracellular domain of β-DG. It is well known that under both, physiological and pathological conditions, gelatinases (*i.e.* MMP-9 and/or MMP-2) can degrade DG, disrupting the connection between the extracellular matrix and the cytoskeleton. However, the molecular mechanisms and the exact cleavage sites underlying these events are still largely unknown. In a previous study, we have characterized the enzymatic digestion of the murine β-DG ectodomain by gelatinases, identifying a main cleavage site on the β-DG ectodomain produced by MMP-9. In this article, we have deepened the pattern of the β-DG ectodomain digestion by MMP-2 by using a combined approach based on SDS-PAGE, Orbitrap, and HPLC-ESI-IT mass spectrometry. Furthermore, we have characterized the kinetic parameters of the digestion of some β-DG ectodomain mutants by gelatinases. © 2012 IUBMB

IUBMB *Life*, 64(12): 988–994, 2012

INTRODUCTION

Dystroglycan (DG) is an ubiquitous membrane glycoprotein complex that includes two subunits, α-DG and β-DG, held together by noncovalent interactions (*1*).

The α-DG subunit adopts a dumbbell-like molecular shape, protruding in the extracellular matrix (ECM), where it preferentially interacts with laminin (*2,3*), whereas the transmembrane β-subunit (43 kDa) is indirectly linked to the actin microfilaments through several macromolecular partners, such as dystrophin and utrophin (*4*). The physiological role of DG has been associated to processes that require intense communication between cells and their microenvironment, such as morphogenesis, tissue development and remodeling (in particular in the nervous and skeletal muscular systems), cell–matrix adhesion, and cell polarization: aberrant degradation of DG indeed is a relevant event in malignancies and in several inflammatory diseases (*5,6*). In this respect, it must be underlined that DG, and in particular the β-subunit, has been proven to be a sensible target of gelatinases, that are, MMP-2 and MMP-9 (*6–9*). Thus, a 30-kDa truncated form of β-DG, devoid of a portion of its extracellular N-terminal domain, has been observed in several tumor cell lines, its formation being associated to the enzymatic activity of gelatinases (*10,11*).

MMP-2 and MMP-9 are matrix metalloproteinases (MMPs), a class of Zn-dependent endopeptidases, which can virtually degrade every macromolecular component of the ECM (*12*). Among these, MMP-2 and MMP-9 show an enzymatic activity associated to a number of relevant physiopathological processes (*13–15*). They considerably differ in their expression profiles: MMP-2 is constitutively released in physiological conditions, whereas MMP-9 is highly inducible. Both enzymes are often expressed in the tumor microenvironment where they contribute

to both malignant transformation and tumor invasiveness by modulating bioavailability of growth factors and by shedding adhesion molecules and basement membrane components (15,16).

We have previously characterized the proteolytic digestion profile of the recombinant β-DG ectodomain, spanning the amino acid residues 654–750, β-DG(654-750), by MMP-9, for which a precise cleavage site has been identified, and by MMP-2, which cleaves the recombinant β-DG ectodomain with higher efficiency (17).

In this article, we extended these studies and documented the cleavage sites in the β-DG ectodomain by MMP-2, using a combined approach based on SDS-PAGE, Orbitrap, and HPLC-ESI-IT mass spectrometry (MS). Furthermore, we have characterized the kinetic parameters for the digestion by gelatinases of some β-DG ectodomain mutants of key residues, mainly involved in the interaction with the α-DG subunit (18,19).

EXPERIMENTAL PROCEDURES

Preparation of the Recombinant Proteins

All the DNA manipulations required for the production of recombinant β-DG, β-DG(654-750), and its mutants have already been described elsewhere (20). Murine β-DG(654-750) recombinant fragments were expressed in *E. coli* BL21(DE3) as thioredoxin fusion proteins, which also contain an N-terminal His6-tag and a thrombin cleavage site, and purified using nickel affinity chromatography. The proteins of interest were obtained upon thrombin cleavage.

Recombinant human full-length pro-MMP-9 was produced in Sf9 insect cells after transfection with a baculovirus carrying the MMP-9 cDNA (21). The secreted pro-MMP-9 was purified by gelatin-sepharose chromatography. The proenzyme was activated by incubating a 10 μM progelatinase solution with a solution containing 0.1 μM of the catalytic domain of MMP-3 (Enzo Life Sciences Inc, Farmingdale, NY, USA) at 37 °C for 90 min. Recombinant human full-length MMP-2 (R&D Systems, Minneapolis, MN, USA) was obtained as a proteolytically active enzyme, thus not requiring any chemical or enzymatic activation. Both these enzymes have been used in previous investigations on different macromolecular substrates (22,23), clearly demonstrating that no contamination by other proteolytic activities was present.

Degradation Assay of β-DG Mutants by Gelatinases

Degradation assays of β-DG(654-750) and its mutants, L716A, F700A, and F718A, with human MMP-2 and MMP-9 were performed at 37 °C in an universal MMP activity buffer (50 mM Tris/HCl, 0.1 M NaCl, 10 mM CaCl₂; pH 7.3).

Each substrate at a final concentration of 15 μM was incubated with 100 nM MMP-2 and 100 nM MMP-9. Aliquots from the reaction mixture were collected and analyzed as previously reported (17).

Determination of the Catalytic Parameters of the F718A Mutant Degradation

Degradation kinetics of the F718A mutant were carried out at different substrate concentrations: 40, 20, 13.5, and 7 μM in the presence of 100 nM MMP-2 or MMP-9. Aliquots were collected at different time intervals and then analyzed. The verification for the applicability of the Michaelis–Menten approximation to the first cleavage step and the determination of the catalytic parameters were undertaken by a global analysis of experimental data according to both the Lineweaver–Burk equation (1) and the Eadie-Hofstee equation (2):

$$\frac{E_0}{v} = \frac{K_m}{k_{cat}} \cdot \frac{1}{[S]} + \frac{1}{k_{cat}}, \tag{1}$$

$$\frac{v}{E_0} = k_{cat} - \frac{v}{E_0 \cdot [S]} \cdot K_m, \tag{2}$$

where E_0 is the total enzyme concentration, v is the actual rate (expressed as M s^{-1}), K_m is the Michaelis–Menten equilibrium constant (expressed as M), k_{cat} is the rate-limiting step kinetic constant (expressed as sec^{-1}), and $[S]$ is the substrate concentration.

RP-HPLC ESI-MS and MS/MS Analyses

High-resolution HPLC-ESI-MS/MS experiments were carried out by an Ultimate 3000 Micro HPLC apparatus (Dionex, Sunnyvale, CA, USA) coupled to a LTQ Orbitrap XL apparatus (ThermoFisher, Scientific, Walthman, MA, USA). The chromatographic column was a Zorbax 300 SB-C18 (3.5 μm particle diameter; column dimension 1 mm i.d. × 15 cm).

High-resolution micro-HPLC-ESI-MS/MS experiments were performed with the following eluents: (A) 0.05% (v/v) aqueous trifluoroacetic acid (TFA) and (B) 0.05% (v/v) TFA in acetonitrile. The applied gradient was 0–4 min 5% B, 4–34 min from 5 to 50% B (linear), and 34–64 min from 50 to 90% B (linear) at a flow rate of 80 μL min^{-1}. In data-dependent acquisition mode, the three most intense multicharged ions were selected and fragmented by using collision-induced dissociation (35% normalized collision energy) and then the spectra were recorded. Alternatively, fragmentation was carried out on selected multicharged ions corresponding to specific protein masses. Tuning parameters were as follows: capillary temperature: 220 °C, source voltage: 2.4 kV, capillary voltage: 26 V, tube lens voltage: 245 V. Experimental mass values were compared with the theoretical average mass (M_{av}) values available at the Swiss-Prot data bank. Data obtained from the micro-HPLC-ESI-MS/MS LTQ Orbitrap XL apparatus were elaborated by the Protein Discovery program, based on SEQUEST cluster as search engine (University of Washington, USA, licensed to Thermo Electron Corp., San Jose, CA, USA) against the Swiss-Prot mouse proteome. For peptide matching, the following limits were used: X_{corr} scores greater than 1.5 for singly charged peptide ions and 2.0 and 2.5 for doubly and triply charged ions,

respectively; peptide mass search tolerance was set to 1.0 Da. The relative abundances of β-DG(654-750) and derivatives were approximately calculated by performing a multiple extracted ion current (XIC) search for every species. The XIC procedure is based on the extraction of the current associated to either one (single XIC) or more (multiple XIC) ions with selected m/z values from the total ion current (TIC) profile. The most relevant m/z values were chosen to have a rough value of the TIC connected to each protein/peptide. Under the constant analytical conditions applied in this study, it was possible to use the integrated ion current peak area for a rough estimation of relative peptide/protein abundances (24).

RESULTS AND DISCUSSION

Identification of MMP-2 Cleavage Sites in Recombinant Mouse β-DG Ectodomain

Proteolytic digestion of 15 μM β-DG ectodomain, β-DG(654-750), by 100 nM MMP-2 was followed by SDS-PAGE. The intensity of the 15 kDa band corresponding to the whole β-DG(654-750) after 3 and 6 h of incubation was markedly reduced (Fig. 1). The process was accompanied by the appearance of lower molecular weight fragments: two major fragments were visible with a molecular mass of about 7 and 12 kDa, as from densitometric analysis of the bands (Fig. 1).

However, Orbitrap MS analysis of the reaction mixtures revealed that the degradation by MMP-2 followed a more complex pattern. The analysis allowed the identification of 32 fragments, whose presence was confirmed by LC-ESI-MS, whereas the relative quantification was carried out following the XIC methods (Table 1).

Three fragments were identified at time 0 (Fig. 2): their relative mass and quantity were determined and reported in Table 1. After 3 h of incubation, the generated fragments pattern appeared complex (Fig. 2 and Table 1): cleavage by MMP-2 occurred at multiple sites, mainly located between the amino acid residues 672 and 750, generating 22 fragments. After 6 h of incubation, the 22 fragments were further processed by MMP-2, generating 32 fragments. The amino acid sequence of the fragments were confirmed by MS/MS (Fig. 3). The β-DG(654-750) cleavage is confirmed to occur randomly in the overall molecule (Fig. 2 and Table 1). It is noteworthy that in the vast majority of the cases, the cleavages take place in correspondence of hydrophobic amino acids. This result is consistent with the notion that nonpolar amino acids are likely to better adapt in the S1 site of the MMP-2 catalytic pocket, and it further reflects a common feature of MMPs behavior (25,26). This proteolytic mechanism is quite different from what observed in a previous study for MMP-9, where the first cleavage event took place between the amino acids His-715 and Leu-716 of the β-DG ectodomain, leading to the formation of a very stable C-terminal fragment (17). The N-terminal fragment, which originated from that first cleavage, was further processed.
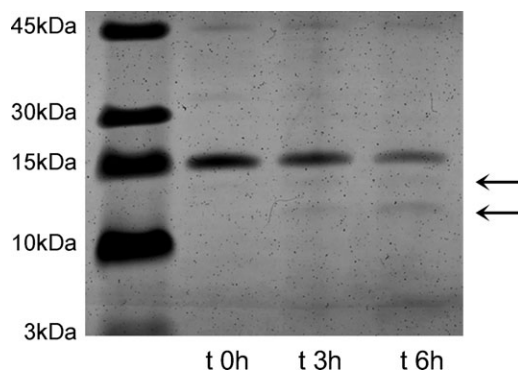

Figure 1. SDS-PAGE analysis of β-DG(654-750) proteolytic digestion by MMP-2. Aliquots were harvested at time 0 and after 3 and 6 h. The intensity of the 15 kDa band corresponding to the whole ectodomain progressively reduces in intensity, whereas it is possible to note the appearance of lower molecular weight fragments especially after 6 h of incubation (black arrows). Samples from the same reaction mixture were analyzed through Orbitrap MS analysis (see Table 1).

Degradation Assay of the β-DG Ectodomain Mutants by Gelatinases

The activity of 100 nM MMP-2 and MMP-9 was investigated on some β-DG(654-750) mutants, namely (a) F700A and F718A, which displayed a reduced affinity toward the C-terminal portion of α-DG (18), and (b) L716A, which alters the MMP-9 main cleavage site (17). Figures 4A–4C show that the F700A and L716A mutants were degraded with the same apparent efficiency by MMP-2 and MMP-9 when compared with wild-type, indicating that the introduced mutations are not sufficient to modulate the enzymatic activity. Conversely, the F718A mutant underwent a more efficient degradation by both gelatinases (Fig. 4D), clearly indicating that a hydrophobic residue at this position might play a protective role for DG against a proteolytic attack. Furthermore, the similar effect for MMP-2 and MMP-9 indeed suggests that the interaction of the two gelatinases with the β-DG ectodomain is modulated in a similar fashion. In particular, the F718A mutation brings about a consistent improvement of the substrate processing, as indicated by a 10-fold enhancement of the catalytic efficiency for MMP-9 [$k_{cat}/K_m = 5.4(\pm0.8) \times 10^3$ M^{-1} s^{-1} for F718A and $k_{cat}/K_m = 6.8(\pm0.8) \times 10^2$ M^{-1}s^{-1} for wild-type β-DG] and a 50-fold increase for MMP-2 [$k_{cat}/K_m = 4.9(\pm0.8) \times 10^5$ M^{-1}s^{-1} for F718A and $k_{cat}/K_m = 8.5(\pm1.3) \times 10^3$ M^{-1}s^{-1} for wild-type β-DG] (see Fig. 4) (17). This effect is completely referable to a dramatic enhancement of the enzymatic affinity toward this mutant, as we observe an increase by about 2 orders of magnitude for MMP-2 and MMP-9 affinity [in the case of MMP-9, $K_m = 3.7(\pm0.2) \times 10^{-6}$ M for F718A and $K_m = 1.4(\pm0.2) \times 10^{-4}$ M for wild-type β-DG, in the case of MMP-2, $K_m = 1.9(\pm0.2) \times 10^{-7}$ M for F718A and $K_m = 4.5(\pm0.6) \times 10^{-4}$ M for wild-type β-DG], whereas k_{cat} is similar to that observed

Table 1

β-DG(654–750) fragments generated by MMP-2

MMP-2 t = 0 h	MMP-2 t = 3 h	MMP-2 t = 6 h	Sequence	MH + [Da]	RT [min]
		1.54E+08	AFSNALEPDFK	1238.607	22.72
		2.20E+08	QIIGLSRRIAD	1241.734	20.67
		1.73E+08	SNALEPDFKALS	1291.655	23.37
		1.06E+08	AFSNALEPDFKA	1309.644	23.56
		1.12E+08	LQFIPVAPPSPGS	1309.717	24.86
		1.51E+08	AFSNALEPDFKAL	1422.729	27.36
1.11E+08	3.51E+09	3.93E+09	RDPEKSSEDDVY	1439.631	13.93
	2.68E+08	1.06E+09	AFSNALEPDFKALS	1509.762	26.22
		1.58E+08	AFSNALEPDFKALSIA	1693.883	29.31
	1.21E+08	3.74E+08	IIGLSRRIADENGKPRP	1892.085	19.84
		1.06E+08	IIGLSRRIADENGKPRPA	1963.122	19.78
	3.57E+08	1.52E+09	QIIGLSRRIADENGKPRP	2020.144	20.49
		2.42E+08	IIGLSRRIADENGKPRPAF	2110.191	22.95
	1.40E+08	5.46E+08	QIIGLSRRIADENGKPRPAF	2238.25	23.25
	1.22E+08	3.46E+08	ENGKPRPAFSNALEPDFKALS	2288.172	25.79
	4.84E+08	6.09E+08	GSSAAPATEVPDRDPEKSSEDDV	2359.053	16.39
	4.01E+08	5.31E+08	SNALEPDFKALSIAVTGSGSCRH	2360.169	27.54
	2.83E+08	6.66E+08	SAAPATEVPDRDPEKSSEDDVY	2378.066	17.68
	1.20E+09	2.50E+09	ENGKPRPAFSNALEPDFKALSIA	2472.293	28.46
	6.99E+08	1.76E+09	GSSAAPATEVPDRDPEKSSEDDVY	2522.118	22.01
	7.08E+08	1.61E+09	AFSNALEPDFKALSIAVTGSGSCRH	2578.277	30.12
	6.20E+07	2.54E+08	ENGKPRPAFSNALEPDFKALSIAVTGSGSCRH	3356.688	29.06
3.12E+07	5.98E+07	2.12E+08	IIGLSRRIADENGKPRPAFSNALEPDFKALS	3382.83	27.16
	6.68E+07	1.21E+08	LQFIPVAPPSPGSSAAPATEVPDRDPEKSSEDD	3406.635	24.19
	8.33E+07	1.03E+08	FIPVAPPSPGSSAAPATEVPDRDPEKSSEDDVY	3427.621	22.46
	8.27E+08	6.71E+08	LQFIPVAPPSPGSSAAPATEVPDRDPEKSSEDDV	3505.706	24.92
		5.54E+08	QIIGLSRRIADENGKPRPAFSNALEPDFKALS	3510.889	27.22
	1.01E+09	2.08E+09	LQFIPVAPPSPGSSAAPATEVPDRDPEKSSEDDVY	3668.764	25.62
	4.77E+08	8.96E+08	IAVTGSGSCRHLQFIPVAPPSPGSSAAPATEVPDRDPEKSSEDDVY	4737.287	25.27
	7.99E+08	8.24E+08	SNALEPDFKALSIAVTGSGSCRHLQFIPVAPPSPGSSAAPATEVPDRDPEKSSEDDVY	6009.927	30.78
	3.02E+09	2.68E+09	AFSNALEPDFKALSIAVTGSGSCRHLQFIPVAPPSPGSSAAPATEVPDRDPEKSSEDDVY	6228.042	32.33
3.11E+08	8.10E+08	7.01E+08	ENGKPRPAFSNALEPDFKALSIAVTGSGSCRHLQFIPVAPPSPGSSAAPATEVPDRDPEKSSEDDVY	7006.438	31.55

Orbitrap MS analysis allowed the identification of 32 fragments derived by MMP-2 proteolytic digestion of β-DG(654–750). The same fragments were also identified by LC-ESI-MS: their relative quantifications at 0, 3, and 6 h were obtained using the XIC method and are reported on the first, second, and third column; the amino acid sequence of each fragment with the monoisotopic mass of the corresponding singly charged peptides (MH+) and its retention time (RT) are reported on the fourth, fifth, and sixth column, respectively.

Figure 2. Time evolution of β-DG(654-750) fragmentation by MMP-2. The β-DG(654-750) fragments generated by proteolytic degradation by MMP-2 are reported in relation to the incubation times. $t = 0$ refers to β-DG(654-750) solution before addition of the enzyme. At $t = 0$, only three fragments (reported in light blue) were detected and MS/MS analyzed by Orbitrap (see Table 1 for relative quantity). After 3 h of incubation, an increased number of fragments was observed (reported in black) mainly deriving by the fragmentation of a portion comprised between the amino acid residues 672 and 750. After 6 h, some smaller fragments appeared (reported in red). [Color figure can be viewed in the online issue, which is available at wileyonlinelibrary.com.]
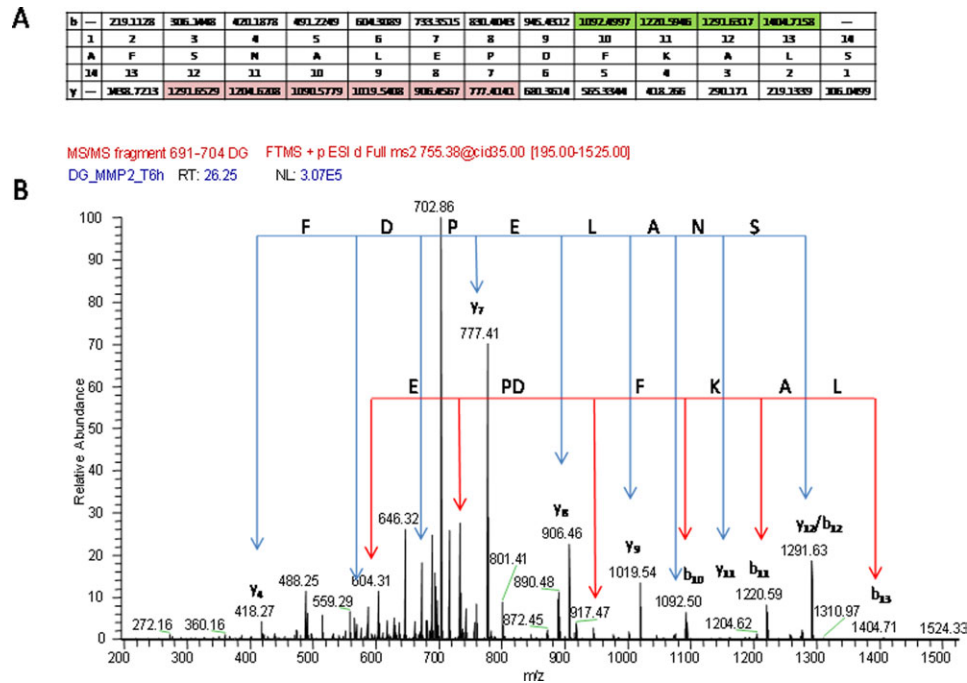
Figure 3. MS/MS fragmentation of a β-DG(654-750) fragment. A representative MS/MS fragmentation of the 691-704 peptide, revealed at time 3 h of the incubation with MMP-2. The theoretical (A) and experimental (B) values for y and b MS/MS ions obtained by the Orbitrap mass spectrometer are reported. [Color figure can be viewed in the online issue, which is available at wileyonlinelibrary.com.]

for wild-type in the case of MMP-9 [$k_{cat} = 0.02(\pm0.01)$ s^{-1} for F718A and $k_{cat} = 0.09\pm(0.01)$ s^{-1} for wild-type β-DG] and even somewhat slower for MMP-2 [$k_{cat} = 0.093(\pm0.01)$ s^{-1} for F718A and $k_{cat} = 3.85(\pm0.53)$ s^{-1} for wild-type β-DG]. This result clearly indicates that the bulky F718 residue represents a major determinant for the interaction of both gelatinases with the β-DG ectodomain, likely because it limits the accessibility, and thus the affinity, of the enzymes to the substrate in the neighborhood of the cleavage site. F718 represents a sort of shield against an indiscriminate cleavage of a "natively unfolded protein", which might be easily cleaved if not adequately protected.

In conclusion, we showed that MMP-2 displays greater affinity and catalytic efficiency on the β-DG ectodomain than MMP-9, producing also a different degradation profile. The intrinsic structural features of the two gelatinases could furnish an explanation for such a divergent interaction with the same substrate. The highly glycosylated OG domain of MMP-9 confers flexibility to the enzyme and makes it suitable to interact with large macromolecular substrates such as collagen (21,27,28), although the OG domain presumably limits the accessibility to small substrates such as the β-DG ectodomain. Therefore, in a pathological context, as in the case of a tumoral microenvironment, the smaller structural arrangement of MMP-2 seems to be more suitable for the β-DG ectodomain breakdown.

Furthermore, we could speculate about the biological significance of these different behaviors: the MMP-2 digestion profile

strongly correlates with extensive breakdown of the β-DG subunit and could be reasonably associated to a mere loss of cell adhesion; on the other hand, the fewer higher molecular weight fragments generated by MMP-9, some of which appear to be particularly stable, likely originate from a non random targeting of the substrate. Such fragments, taking into consideration the
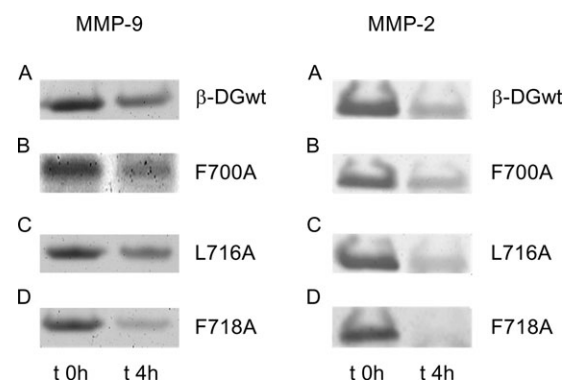

Figure 4. Comparison of proteolytic digestion of β-DG mutants. Proteolytic digestion of β-DG(654-750) (A) and its mutants, F700A (B), L716A (C), and F718A (D) by MMP-2 or MMP-9. Small aliquots from the reaction mixture were collected before the incubation ($t = 0$) and 4 h later ($t = 4$ h). The disappearance of the 15 kDa band corresponds to the degradation of the whole β-DG(654-750) or its mutants.

restricted spatial and chronological pattern of expression of the enzyme, could intriguingly be part of a still unknown signaling cascade, a possibility already envisaged for the β-DG subunit (29) and common to several ECM substrates of MMPs. In this respect, multiple mutants of β-DG putative cleavage sites might be useful in casting some additional light onto the enzymatic mechanism.

ACKNOWLEDGEMENTS

REFERENCES

1. Ibraghimov-Beskrovnaya, O., Ervasti, J. M., Leveille, C. J., Slaughter, C. A., Sernett, S. W., et al. (1992) Primary structure of dystrophin-associated glycoproteins linking dystrophin to the extracellular matrix. *Nature* **355**, 696–702.

2. Bozzi, M., Morlacchi, S., Bigotti, M. G., Sciandra, F., and Brancaccio, A. (2009) Functional diversity of dystroglycan. *Matrix Biol.* **28**, 179–187.

3. Henry, M. D. and Campbell, K. P. (1999) Dystroglycan inside and out. *Curr. Opin. Cell Biol.* **11**, 602–607.

4. Barresi, R. and Campbell, K. P. (2006) Dystroglycan: from biosynthesis to pathogenesis of human disease. *J. Cell Sci.* **119**, 199–207.

5. Court, F. A., Zambroni, D., Pavoni, E., Colombelli, C., Baragli, C., et al. (2011) MMP2-9 cleavage of dystroglycan alters the size and molecular composition of Schwann cell domains. *J. Neurosci.* **31**, 12208–12217.

6. Sgambato, A. and Brancaccio, A. (2005) The dystroglycan complex: from biology to cancer. *J. Cell Physiol.* **205**, 163–169.

7. Agrawal, S., Anderson, P., Durbeej, M., van Rooijen, N., Ivars, F., et al. (2006) Dystroglycan is selectively cleaved at the parenchymal basement membrane at sites of leukocyte extravasation in experimental autoimmune encephalomyelitis. *J. Exp. Med.* **203**, 1007–1019.

8. Michaluk, P., Kolodziej, L., Mioduszewska, B., Wilczynski, G. M., Dzwonek, J., et al. (2007) β-Dystroglycan as a target for MMP-9, in response to enhanced neuronal activity. *J. Biol. Chem.* **282**, 16036–16041.

9. Zhao, X. L., Li, G. Z., Sun, B., Zhang, Z. L., Yin, Y. H., et al. (2010) MMP-mediated cleavage of β-dystroglycan in myelin sheath is involved in autoimmune neuritis. *Biochem. Biophys. Res. Commun.* **392**, 551–556.

10. Losasso, C., Di Tommaso, F., Sgambato, A., Ardito, R., Cittadini, A., et al. (2000) Anomalous dystroglycan in carcinoma cell lines. *FEBS Lett.* **484**, 194–198.

11. Zhong, D., Saito, F., Saito, Y., Nakamura, A., Shimizu, T., et al. (2006) Characterization of the protease activity that cleaves the extracellular domain of β-dystroglycan. *Biochem. Biophys. Res. Commun.* **345**, 867–871.

12. Nagase, H. and Woessner, J. F., Jr. (1999) Matrix metalloproteinases. *J. Biol. Chem.* **274**, 21491–21494.

13. Van den Steen, P. E., Dubois, B., Nelissen, I., Rudd, P. M., Dwek, R. A., et al. (2002) Biochemistry and molecular biology of gelatinase B or matrix metalloproteinase-9 (MMP-9). *Crit. Rev. Biochem. Mol. Biol.* **37**, 375–536.

14. Li, H., Mittal, A., Makonchuk, D. Y., Bhatnagar, S., and Kumar, A. (2009) Matrix metalloproteinase-9 inhibition ameliorates pathogenesis and improves skeletal muscle regeneration in muscular dystrophy. *Hum. Mol. Genet.* **18**, 2584–2598.

15. Sbardella, D., Fasciglione, G. F., Gioia, M., Ciaccio, C., Tundo, G. R., et al. (2012) Human matrix metalloproteinases: an ubiquitarian class of enzymes involved in several pathological processes. *Mol. Aspects Med.* **33**, 119–208.

16. Björklund, M. and Koivunen, E. (2005) Gelatinase-mediated migration and invasion of cancer cells. *Biochim. Biophys. Acta* **1755**, 37–69.

17. Bozzi, M., Inzitari, R., Sbardella, D., Monaco, S., Pavoni, E., et al. (2009) Enzymatic processing of β-dystroglycan recombinant ectodomain by MMP-9: identification of the main cleavage site. *IUBMB Life* **61**, 1143–1152.

18. Bozzi, M., Veglia, G., Paci, M., Sciandra, F., Giardina, B., et al. (2001) A synthetic peptide corresponding to the 550–585 region of α-dystroglycan binds β-dystroglycan as revealed by NMR spectroscopy. *FEBS Lett.* **499**, 210–214.

19. Bozzi, M., Sciandra, F., Ferri, L., Torreri, P., Pavoni, E., et al. (2006) Concerted mutation of Phe residues belonging to the β-dystroglycan ectodomain strongly inhibits the interaction with α-dystroglycan in vitro. *FEBS J.* **273**, 4929–4943.

20. Di Stasio, E., Sciandra, F., Maras, B., Di Tommaso, F., Petrucci, T. C., et al. (1999) Structural and functional analysis of the N-terminal extracellular region of β-dystroglycan. *Biochem. Biophys. Res. Commun.* **266**, 274–278.

21. Van den Steen, P. E., Van Aelst, I., Hvidberg, V., Piccard, H., Fiten, P., et al. (2006) The hemopexin and O-glycosylated domains tune gelatinase B/MMP-9 bioavailability by inhibition and binding to cargo receptors. *J. Biol. Chem.* **281**, 18626–18637.

22. Gioia, M., Monaco, S., Fasciglione, G. F., Coletti, A., Modesti, A., et al. (2007) Characterization of the mechanism by which gelatinase A, neutrophil collagenase and membrane-type metalloproteinase MMP-14 recognize collagen I and enzymatically process the two α-chains. *J. Mol. Biol.* **368**, 1101–1113.

23. Gioia, M., Monaco, S., Van den Steen, P. E., Sbardella, D., Grasso, G., et al. (2009) The collagen binding domain of gelatinase A modulates degradation of collagen IV by gelatinase B. *J. Mol. Biol.* **386**, 419–434.

24. Ong, S. E. and Mann, M. (2005) Mass spectrometry-based proteomics turns quantitative. *Nat. Chem. Biol.* **1**, 252–262.

25. Van den Steen, P. E., Proost, P., Grillet, B., Brand, D. D., Kang, A. H., et al. (2002) Cleavage of denatured natural collagen type II by neutrophil gelatinase B reveals enzyme specificity, post-translational modifications in the substrate, and the formation of remnant epitopes in rheumatoid arthritis. *FASEB J.* **16**, 379–389.

26. Chen, E. I., Li, W., Godzik, A., Howard, E. W., and Smith, J. W. (2003) A residue in the S2 subsite controls substrate selectivity of matrix metalloproteinase-2 and matrix metalloproteinase-9. *J. Biol. Chem.* **278**, 17158–17163.

27. Overall, C. M. and Butler, G. S. (2007) Protease yoga: extreme flexibility of a matrix metalloproteinase. *Structure* **15**, 1159–1161.

28. Rosenblum, G., Van den Steen, P. E., Cohen, S. R., Grossmann, J. G., Frenkel, J., et al. (2007) Insight into the structure and domain flexibility of full-length pro-matrix metalloproteinase-9/gelatinase B. *Structure* **15**, 1227–1236.

29. Moore, C. J. and Winder, S. J. (2010) Dystroglycan versatility in cell adhesion: a tale of multiple motifs. *Cell Commun. Signal.* **8**, 3–14.